LAWRENCE
LIVERMORE
NATIONAL
LABORATORY

LLNL-TR-707598

Prototype Stilbene Neutron Collar

M. K. Prasad, D. Shumaker, N. Snyderman, J. Verbeke, J. Wong

October 31, 2016

Disclaimer

This work performed under the auspices of the U.S. Department of Energy by Lawrence Livermore National Laboratory under Contract DE-AC52-07NA27344.

Prototype Stilbene Neutron Collar

by

Manoj Prasad, Dan Shumaker, Neal Snyderman,
Jerome Verbeke, and James Wong

Lawrence Livermore National Laboratory,
Livermore CA 94550, USA
October 2016

Abstract

A neutron collar using stilbene organic scintillator cells for fast neutron counting is described for the assay of fresh low enriched uranium (LEU) fuel assemblies. The prototype stilbene collar has a form factor similar to standard He-3 based collars and uses an AmLi interrogation neutron source. This report describes the simulation of list mode neutron correlation data on various fuel assemblies including some with neutron absorbers (burnable Gd poisons). Calibration curves (doubles vs ^{235}U linear mass density) are presented for both thermal and fast (with Cd lining) modes of operation. It is shown that the stilbene collar meets or exceeds the current capabilities of He-3 based neutron collars. A self-consistent assay methodology, uniquely suited to the stilbene collar, using triples is described which complements traditional assay based on doubles calibration curves.

1. Introduction

We report here the details of a prototype neutron collar design based on stilbene scintillator crystals which count fast neutrons. This work was done for the NA-241 Safeguards Technology group Neutron Detector Rodeo Project in FY16. The goal of the project was to compare and evaluate several detector material alternatives to He-3 for quantifying fissile Uranium in fresh fuel. The IAEA currently uses the Uranium Neutron Coincidence Collar (UNCL) for this application. The UNCL is used to determine the linear mass density of ^{235}U in fresh fuel assemblies. The instrument is cart-portable and consists of 18 He-3 tubes embedded in a polyethylene collar and includes an AmLi interrogation neutron source which is also embedded in the poly. Details of the assay technique are described in Ref [1] and a description of the commercially available He-3 based UNCL can be found in Ref [2].

The prototype stilbene neutron collar design described here has a form factor similar to the UNCL and meets or exceeds the current capabilities of the UNCL. We also discuss a self-consistent assay methodology that is uniquely suited to the prototype stilbene neutron collar and which complements the traditional assay technique described in Ref [1].

2. Benefits of Stilbene for Fast Neutron Collar Detector

A fuel assembly is typically interrogated with an AmLi neutron source that is moderated by being embedded in a block of polyethylene. The thermalized AmLi neutrons have a high probability of inducing fission in the ^{235}U component of the fuel assembly and therefore allow an assay of the ^{235}U content along the axis of the assembly. With standard He-3 based neutron collar, the thermalized AmLi interrogating neutron source drowns the signal from the induced fission on ^{235}U. A neutron collar based on stilbene will be almost blind to the thermalized interrogating neutron source since it is a threshold detector that only sees neutrons exceeding some energy threshold of 0.5 to 1 MeV. Therefore, a stilbene based neutron collar will clearly see the induced fission on ^{235}U without being

blinded by the interrogating source. The improved S/N (signal-to-noise) of stilbene is a key motivation for using stilbene. Typically, only 20% of the count rate in a He-3 based collar is from the fuel assembly whereas for a stilbene collar 90% of the count rate is from the assembly.

Stilbene, like all scintillator based neutron detectors, has a fast response time on the order of a nano-second compared to He-3 based detectors with characteristic response times of several tens of micro-seconds. This fast response time can resolve individual fission chains (bursts) and permit a detailed analysis of the underlying neutron multiplication. The fast response time permits a much shorter timegate (measurement time window) for counting neutrons and their correlations with very few 'accidentals'. This leads to an accurate and rapid assay in significantly lower measurement times.

Since a fast 1MeV neutron travels at 1.5cm/ns, with nano-second time resolution it is possible to resolve the spatial distribution of SNM (special nuclear material) at cm scales using neutron and gamma correlations. While this is not a requirement for the neutron rodeo it is an important capability of fast neutron counting to be aware of that can potentially be used to great advantage.

With scintillator based detection what is actually being measured is the scintillator light output spectrum. From this light output spectrum one can unfold the neutron energy spectrum of the neutrons being detected. Depending on the source of neutrons, the neutron energy spectrum can vary significantly. Neutrons from a spontaneous fission source have distinctively different spectrum compared to neutrons from (α,n) sources. This allows us to infer the alpha ratio A = [(α,n) source rate]/[spontaneous fission source rate] which in general is a challenging parameter to assay. Stilbene based collars can provide insight into the alpha ratio.

Finally, stilbene is an optimal scintillator detector because it has the highest organic scintillation efficiency with much higher light yield than plastics or liquids. It has an excellent PSD (pulse shape discrimination) which allows for excellent gamma rejection which in turn implies high neutron detection efficiency. This high efficiency is critical to it being competitive with He-3 based neutron detectors.

LLNL researchers (Ref [3, 4]) pioneered the rapid, safe solution growth of stilbene crystals. This technology is licensed to Inrad Optics (Ref [5]) through which large stilbene crystals (4” diameter x 2” depth) are commercially available. The prototype stilbene neutron collar design described here uses 30 of these 4”x2” crystals that can fit into the form factor of standard He-3 based collar, as shown in Fig. 1 below:

LLNL Prototype Stilbene ($C_{14}H_{12}$) Neutron Collar Detector:
3 panels, each with 10 cells
Each cell 9cm diameter, 6cm depth, ρ =1.15 g/cc
Each panel 8.34” (D) x 9.92” (W) x 15.8” (H)

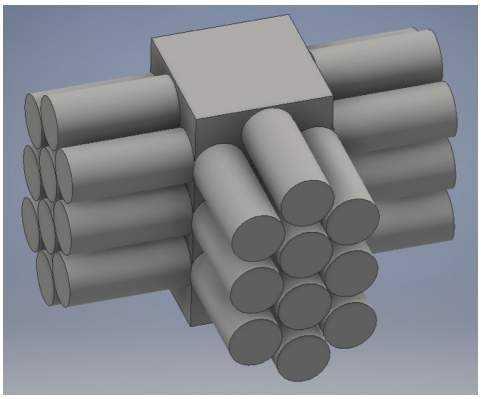

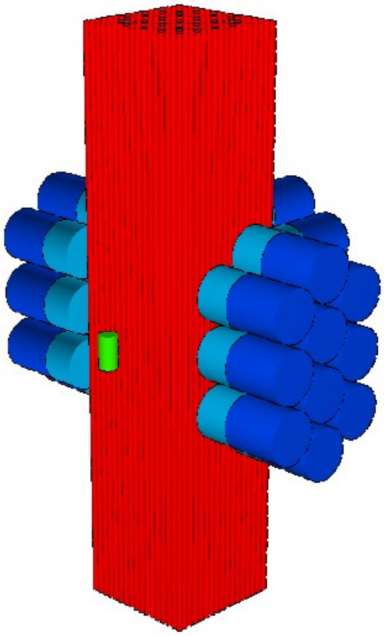

Fig1. LLNL prototype stilbene neutron collar with 30 stilbene cells and a form factor similar to commercially available He-3 based UNCL. Also shown is a MCNP model of the stilbene collar with a fuel assembly and an AmLi interrogating neutron source (shown without the poly bank in which it is embedded).

A flow chart of the stilbene detector hardware and data acquisition is shown in Fig.2:

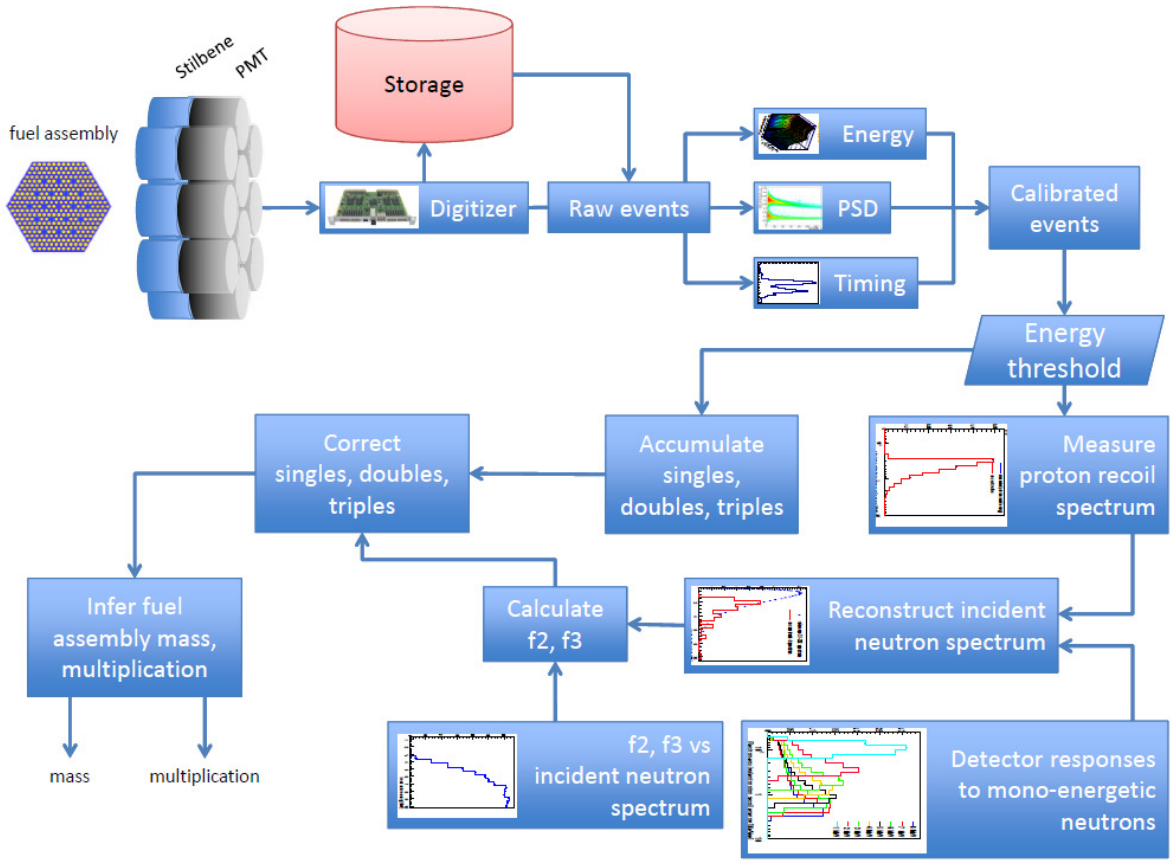

Fig2. Prototype stilbene neutron collar detector hardware and data acquisition

3. Neutron Energy Spectrum N(E): Fast & Thermal Modes

Stilbene is a fast neutron detector that only detects neutrons above a certain threshold energy. It is therefore important to understand the neutron energy spectrum arising from the AmLi interrogating source and its coupling with the fuel assembly. There are two modes of operation for a neutron collar: fast mode and thermal mode. In fast mode a thin (0.5 mm) lining of Cd is put around the fuel

cavity to filter out neutrons below the Cd cutoff energy (0.5 eV) from entering the fuel assembly. This is important in the assay of poisoned fuel rods (with Gd doping) that can absorb low energy neutrons. Traditional assay is based on 'calibration' curves of doubles vs. ^{235}U linear density (in g/cm) which are vulnerable to neutron absorption effects. A calibration curve in fast mode will be immune to distortions from neutron absorption.

The Obninsk AmLi interrogating neutron source used for the neutron rodeo has a unique neutron energy spectrum N(E) as shown below:

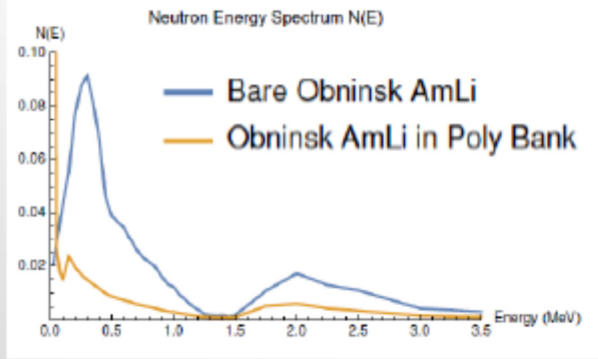

Fig3. Neutron Energy Spectrum N(E) of bare and moderated (by being embedded in poly bank) Obninsk AmLi interrogating neutron source.

There is a noticeable bump in the spectrum around 2 MeV arises from O(α,n) reaction on oxygen in the AmO2 and LiOH mixture that comprise the AmLi source (Ref [6]). Typical Li(α,n) reaction spectrum terminates at 1.5 MeV while the Obninsk spectrum has around 5% of neutrons above 1.5 MeV in energy. The effect on the bare Obninsk AmLi neutron energy spectrum by being embedded in the poly bank of the neutron collar is also shown in Fig. 3 and it is evident that most of the neutrons have thermalized with less than 5% of the neutrons above 1 MeV in energy. This neutron energy spectrum was calculated using MCNP with a F4 tally averaged over the 30 stilbene cells where the cells were replaced by void.

In Fig. 4 below we show the neutron energy spectrum as seem by the 30 stilbene cells for the Obninsk AmLi source embedded in the poly bank interrogating a standard 15x15 fuel assembly with ^{235}U linear density of 23.8 g/cm. In Fig. 4 we show both the fast (with 0.5mm Cd lining) and thermal (no Cd lining) modes

neutron energy spectrum for the empty cavity and the 15x15 fuel assembly in the cavity. For comparison purpose, we also show the neutron energy spectrum of a point Cf source (source strength of 34000 n/s) at the center of the cavity. Since the Cf source is a spontaneous fission source of fast neutrons the Cd lining has no effect on the energy spectrum as seen by the stilbene cells.

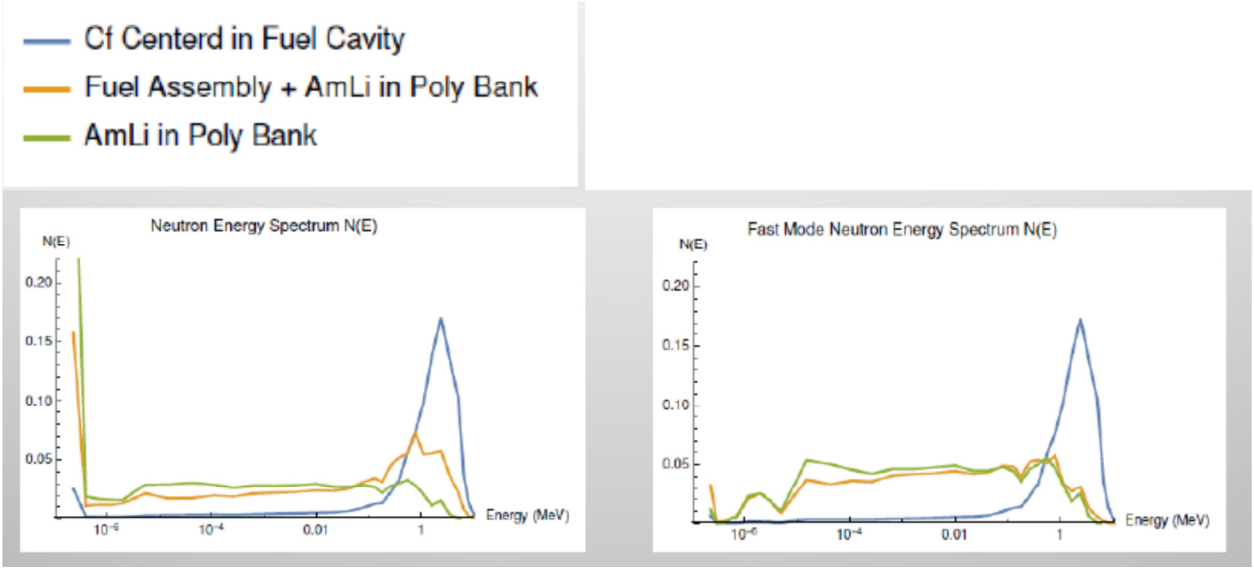

Fig4. Neutron Energy Spectrum N(E) of Cf, fuel assembly with AmLi in poly bank, empty cavity with AmLi in poly bank in thermal and fast modes.

The LEU fuel assembly is mostly ^{238}U which has a large (n,n') inelastic scattering cross section of 3b at 1MeV neutron energies (compared to a fission cross section of 1b on ^{235}U). This means that any fission neutron originating in the fuel assembly may significantly lose energy on its way to being detected by the stilbene to the point that its energy may drop below the threshold for being detected! Fig. 4 shows the neutron energy spectrum resulting from the (n,n') moderation of neutrons along with other physical processes. It is evident that the spectrum is much flatter compared to the Cf source. The end effect of this is a penalty in detection efficiency for the stilbene collar compared to a He-3 based collar. Stilbene with its excellent PSD can make up for this potential loss in efficiency by operating at low PSD threshold of 60 keVee which would not be possible with a liquid scintillator for example. Stilbene based neutron collar can therefore be competitive with a He-3 based collar.

4. Stilbene Scintillation Light Output Spectrum N(L)

The light output from a stilbene cell from a proton recoil energy of Ep was studied by Hansen and Richter in Ref [7]. Their published results for the electron-equivalent light output L (quench function) and angle dependent anisotropy correction factor are:

Light Output :

$$L\ (\text{MeVee}) = 0.693\ E_p - 3\left[1 - e^{-0.2\ E_p^{0.965}}\right]$$

E_p = proton recoil energy (MeV)

Angle Dependent Anisotropy Correction :

$$KF\ (\theta,\ E_p) = 1 + (0.296 - 0.0091\ E_p)\ \sin^2(\theta)$$

$\theta \equiv$ Angle between neutron incidence direction and stilbene crystal axis

We use the Hansen-Richter quench function to generate the stilbene light output spectrum by post-processing our custom LLNL MCNPX simulations of the neutron collar. In the post-processing we use a dead time of 1 micro-second per stilbene cell and a pulse integration time of 15 ns (Ref [9]).

The simulated neutron light output spectrum N(L) for thermal mode is:

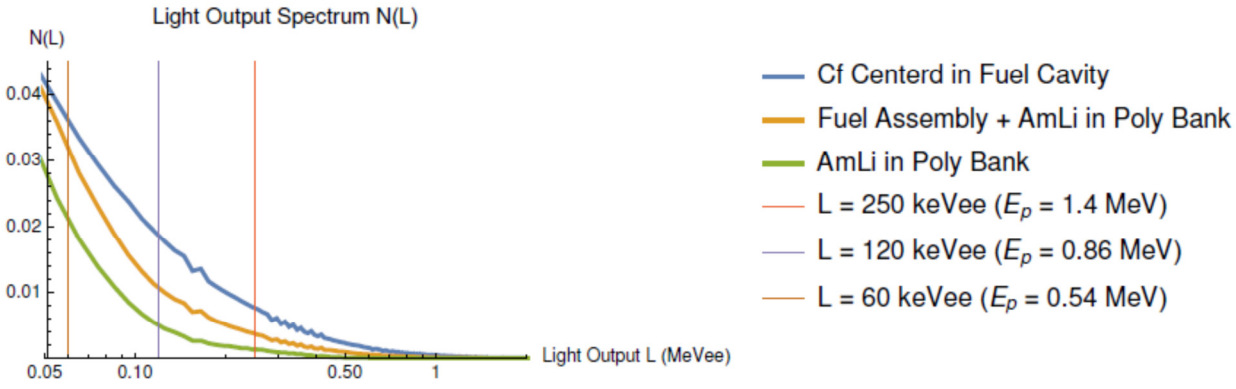

and for fast mode is:

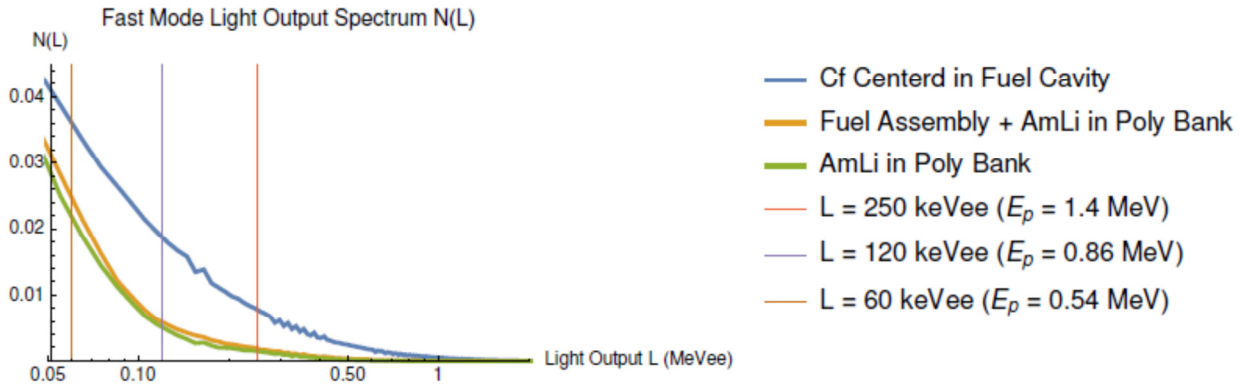

where we have indicated three levels of PSD thresholds (60 keVee, 120 keVee and 250 keVee) that we can operate at. Because of stilbene's excellent PSD we believe that we can operate at 60 keVee to maximize neutron detection efficiency. In contrast, we typically operate our liquid scintillators at 250 keVee.

As described in Ref [11, 12] we can invert the neutron energy spectrum N(E) from the scintillator light output spectrum N(L) along with the multiple scatter corrections as described in Section 7. The inversion is only possible for energies above the scintillator PSD threshold energy. This ability to infer the neutron energy spectrum N(E) is a valuable feature of stilbene detectors, particularly because we can operate stilbene at a low PSD threshold of 60 keVee which corresponds to 0.54 MeV proton recoil energy.

5. List Mode Data: Random & Triggered Counting Distributions

Our modeling of the prototype stilbene neutron collar is based on the simulation of list mode data that records the exact time when a neutron is detected by the neutron detector. From this list mode data we can construct various counting distributions and their correlated moments which can be used for assay. In general we can analyze the time interval between successive or skipped counts in the list mode data. The theory of time interval distributions in list mode data is described in Ref [8] and we will focus here on the results pertaining to two ways of constructing counting distributions: random and triggered counting.

The first way to construct a counting distribution from list mode data is using a random timegate T (Feynman) counting. The list mode data is cut up into N segments, each of length T, and the resulting segments are tallied to see how many segments had so many counts. The random counting distribution is defined as: $b_k(T)$ = (# of segments with k events)/N. A plot of $b_k(T)$ vs. k would look like:

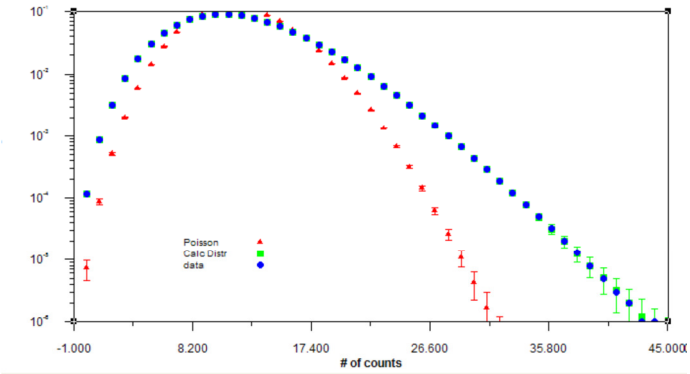

The mean and the Feynman 2nd moment of the b distribution are defined through:

Mean of $b_k(T)$ = R1*T, R1 = Count Rate (Singles)

Feynman Y2F(T) = (Variance – Mean)/(2*Mean) of $b_k(T)$

The second way to construct a counting distribution from the list mode data is using a triggered timegate T (shift-register coincidence) counting. At each event of the list mode data, we open a segment of length T and tally the resulting segments to see how many segments had so many counts. The triggered counting distribution is defined as:

$n_k(T)$ = (# of segments with k events)/(total number of counts)

For a random (Poisson) counting list mode data the random and triggered counting distributions are equal to each other. In general there is an exact mathematical relation between $n_k(T)$ and $b_k(T)$:

$$n_k(T) = \frac{1}{R_1}\frac{d}{dT}\sum_{j=(k+1)}^{\infty} b_j(T)$$

and their (k^{th} factorial moments)/k! $\equiv M_k$:

$$M_k^n(T) = \frac{1}{R_1}\frac{d}{dT}M_{k+1}^b(T)$$

We use a custom MCNPX developed at LLNL to simulate list mode data for both He-3 neutron capture and scintillator neutron scattering counts. Details of this custom LLNL MCNPX27e are described in Ref [9]. Our simulations with the custom MCNPX27e use the LLNL fission library by setting fism=5 in the 6^{th} entry of the PHYS:N card. This setting samples a full measured distribution for the number of fission neutrons emitted in a fission event. The timestamps recorded by the custom LLNL MCNPX27e are in double precision, in contrast to the default MCNP PTRAC which uses single precision. This double precision is especially important when simulating fast neutron detector counting with sub nano-second time resolution to avoid false correlations.

6. Point Model Count Rate R1, Feynman R2F, Doubles

Within the context of a 0-D point model, it is possible to quantify the various moments of the counting distributions in terms of the fundamental SNM (special nuclear material) parameters (Ref [10]):

$S_f \equiv$ Spontaneous Fission Source Rate (neutrons/sec)
M = Total Multiplication from Induced Fission Chain = $1/(1-k_{eff})$
p ≡ Probability for induced fission, $k_{eff} = p\nu$
ν ≡ Average number of neutrons created in an induced fission event
ε ≡ Detection efficiency
A ≡ Alpha ratio ≡ [(α,n) Source Rate]/S_f

As a corollary, the measured moments of the count distribution data can be inverted to infer the fundamental SNM parameters to constitute an assay of the system being measured.

The count rate R1 is given by:

$$\text{Count Rate} = S_f \epsilon (1\text{-}p)\, M\, (1 + A)$$

and the Feynman 2nd moment by:

$$Y2F = R2F\left(1 - \frac{1 - e^{-\lambda T}}{\lambda T}\right)$$

$$R2F = (\epsilon q M)\left[\frac{D_{2\,s}}{(1 + A)} + (M - 1)\, D_2\right]$$

where λ ≡1/(neutron lifetime) ≡ 1/(die-away time)
q ≡1-p ≡ leakage/absorption (non fission) probability
D_{2S}/D_2 are Diven's nuclear constants specific to a SNM Source/Multiplier

The product (qM) in the above formulas is the net multiplication in contrast to the total multiplication M:

Net Multiplication ≡ qM = (1-p)M = M – (M-1)/v
where (M-1)/v = Average number of fissions
qM = (Total number of neutrons created) – (Number of neutrons lost to fission)

The Feynman and shift-register doubles are defined by (Ref [10]):

Feynman Doubles $D_F \equiv$ R1 * R2F

Shift-Register Doubles ≡ **R1* Mean of [$n_k(T)$ - $b_k(T)$]** ≡ D_{SR} = GUF(T) * D_F
GUF(T) = Gate-Utilization-Factor $= e^{-\lambda PreDelay}(1 - e^{-\lambda T})$

For ^{3}He Detectors: PreDelay = 4.5 μs, Gate T = 64 μs,
with Typical DieAway ≈ 50-70 μs, GUF ≈ 0.6

The triggered shift-register moments can be derived from derivatives of the random Feynman moments. From now on, unless otherwise indicated, moments will be assumed to be random Feynman moments and pre-delay = 0.

We quantify correlation by R2F. For a random source of neutrons R2F = 0. For a non-multiplying (M = 1) ^{252}Cf spontaneous fission source R2F = 1.6 ε. A measurement of a ^{252}Cf source R2F is used to define the efficiency ε of a neutron detector through ε= R2F/1.6.

7. Multiple Scattering Crosstalk Correction for List Mode Data

The point model equations of the previous section rely on the assumption that each neutron in the system can be detected only once. This is certainly true for a He-3 based detector because the He-3 captures the neutron and the neutron disappears. It is different with a scintillator based detector, because neutrons in such a system deposit energy in scintillators by scattering with the atoms, and are not absorbed in the elastic and inelastic scattering collisions. They keep traveling, and if they still have enough energy, they can potentially deposit this energy in adjacent or even remote scintillator cells. This multiple scattering crosstalk between scintillator cells must be corrected for in the list mode data.

We have developed a theoretical model for correcting multiple scattering crosstalk in Ref [11]. The model introduces parameters f2 and f3 which are the fractions of neutrons that were detected twice and thrice respectively. Based on these parameters the model shows that the corrupted measured moments are related to the true (no multiple scattering crosstalk) moments through the following simple algebraic equations:

$$R1 = \left(1 + f_2 + 2\,f_3\right) R1^{true}$$

$$R2F = \frac{f_2 + 3\,f_3}{1 + f_2 + 2\,f_3} + \left(1 + f_2 + 2\,f_3\right) R2F^{true}$$

$$R3F = \frac{f_3}{1 + f_2 + 2\,f_3} + 2\left(f_2 + 3\,f_3\right) R2F^{True} + \left(1 + f_2 + 2\,f_3\right)^2 R3F^{true}$$

There are several ways to estimate the parameters f2 and f3. From a forward modeling point of view one can replace the fuel assembly and its moderated AmLi interrogating neutron source by a random source of neutrons with exactly the same neutron energy spectrum as the actual fuel assembly with the AmLi source as shown in Fig. 4. Since the random source of neutrons is uncorrelated $R2F^{true}$ = $R3F^{true}$ = 0 and any simulated R2F and R3F can be attributed to multiple scatter crosstalk. We can use the above algebraic equations to solve for f2 and f3. This forward modeling estimate of f2 and f3 is in general not applicable since in general we do not have a detailed model of what we are measuring.

We have developed, as described in Ref [11, 12], an inverse modeling approach to estimate f2 and f3 from measured data of general unknown objects. The flow chart for this inverse modeling approach is as follows:

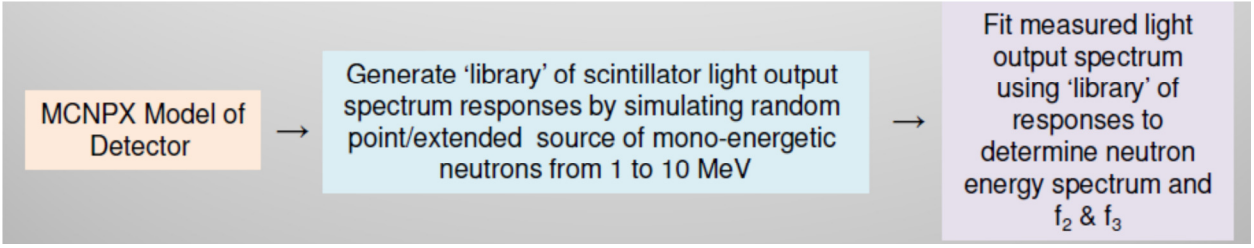

We first develop a detailed MCNPX model of the stilbene scintillator neutron collar detector and generate a library of scintillator light output spectrum N(L) for a set of random point or extended source of mono-energetic neutron with energies ranging from 1 to 10 MeV. We then fit the measured scintillator light output spectrum N(L) with the library of responses to determine the neutron energy spectrum along with f2 and f3 simultaneously.

For the standardized set of fuel assemblies that we modeled for the neutron rodeo both the forward and inverse modeling approaches gave similar estimates for f2 and f3, within 15% of each other. Once we have f2 and f3 we can correct the measured corrupted moments to determine the true moments by using the simple algebraic equations above. We believe this approach to multiple scatter crosstalk correction is much more robust and satisfying than an ad-hoc arbitrary rejection of adjacent events in the list mode data within some rejection time window that is widely used. In fact one can use our inverse modeling approach to

optimize the rejection time window so that the filtered list mode data gives the same f2 and f3 as our inverse modeling. Thus our inverse modeling approach provides a physical model to optimally filter list mode data to correct for multiple scatter crosstalk.

8. ^{252}Cf Spontaneous Fission Source at Center of Neutron Collar

We first simulated a ^{252}CF spontaneous fission source at the center of the neutron collar to determine a nominal efficiency that we can attribute to the collar. The simulation was done for both the standard commercial He-3 neutron collar and our prototype stilbene neutron collar. A cross section of both collars that were modeled is shown below:

We used or custom LLNL MCNPX27e to simulate 10 minutes of list mode data for a 1.453e-8 g of ^{252}Cf (34000n/s) point source. The simulation results that were obtained are:

Neutron Collar	Count Rate R1 (cps)	Die-Away Time 1/λ	Feynman R2F	Inferred Efficiency ε (R2F/1.596)
^{3}He	3575	55.3 µs	0.1596	10%
SB 60 keVee Thermal Mode f_2=0.028 f_3=3.11e-4	5249	4.5 ns	0.2358	14.8%
SB 60 keVee Fast Mode f_2=0.028 f_3=3.05e-4	5234	4.4 ns	0.2353	14.7%

Since the ^{252}Cf neutron source is a fast neutron source both the thermal mode and fast mode (with Cd lining) give similar results. Our prototype stilbene neutron collar has a nominal efficiency of around 15% that is significantly above the corresponding efficiency of 10% for the He-3 neutron collar.

9. Standard Fuel Assembly UNCL_15x15 in Neutron Collar Cavity

We then simulated the standard fuel assembly UNCL_15x15 with a ^{235}U linear density of 23.8 g/cm that was provided for the neutron rodeo. We again used or custom LLNL MCNPX27e to simulate 10 minutes of list mode data with the Obninsk AmLi interrogating neutron source moderated by the poly bank for both the standard He-3 neutron collar and our prototype stilbene neutron collar. A cross section of both collars that were modeled is shown below:

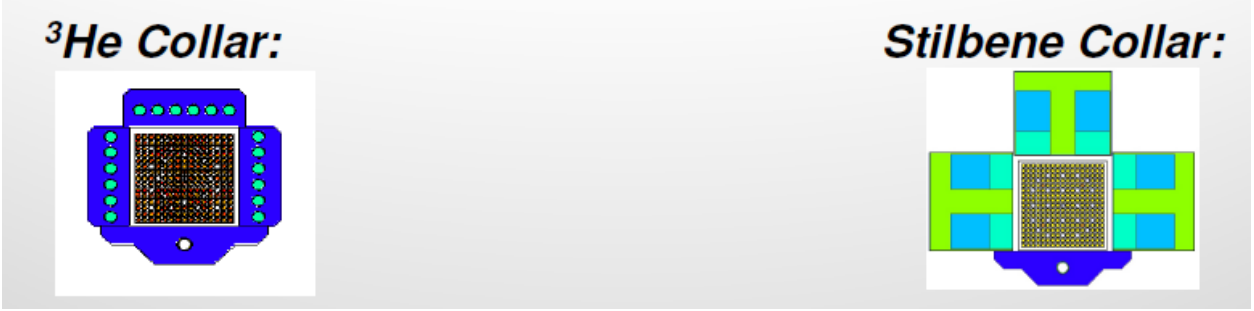

The simulation results that were obtained are:

Neutron Collar	Count Rate R1 (cps)	Die-Away Time 1/λ	Feynman R2F	Feynman Doubles
^{3}He	1882	71.9 µs	0.1179	222
SB 60 keVee Thermal Mode f_2=0.0206 f_3=1.75e-4	943	8 ns	0.1164	110
SB 60 keVee Fast Mode f_2=0.015 f_3=1.0e-4	174	9.4 ns	0.0597	10

We see that the stilbene neutron collar at a PSD threshold of 60 keVee gives a Feynman R2F similar to that of He-3 neutron collar in thermal mode. Unlike the Cf point source case where the stilbene collar was 50% more efficient than the He-3 collar, the (n,n') ineleastic scattering of fission neutrons in 238U reduces the energy of those fission neutrons making stilbene less efficient in detecting those neutrons compared to He-3. However, at 60 keVee threshold the efficiencies for the He-3 collar and stilbene collar are similar. This shows why stilbene is an optimal scintillator detector that can compete with He-3 because only with stilbene can we operate at a low PSD threshold of 60 keVee. By comparison, we typically operate liquid scintillators at a PSD threshold of 250 keVee which would be much less efficient.

For fast mode (with Cd lining) the Feynman R2F, and therefore the effective efficiency, of the stilbene collar (and also for He-3 collar) drops almost by a factor of 2 compared to thermal mode. This is because the neutrons entering the fuel assembly are above the Cd cutoff energy of 0.5 eV and therefor have a much smaller cross section of a few barns to induce fission on the ^{235}U component of the fuel assembly. In thermal mode, the thermal neutrons have a huge cross section of 580 b to induce fission on ^{235}U.

10. Thermal Mode Simulation Results for Neutron Rodeo Project

The neutron rodeo project required us to simulate the prototype stilbene neutron collar on various assemblies:

Calibration assemblies
Unpoisoned Intact Assemblies
Partial Defect Assemblies
Burnable Poison Assemblies

and compare our results with the standard He-3 neutron collar using an Excel spread sheet developed by Anthony Belian (Ref [13]).

In Appendix 1 we present detailed tables of our simulation results in thermal mode (and also in fast mode) for all of the assemblies along with the 252Cf point source and an empty cavity with no fuel assembly but with the moderated Obninsk AmLi neutron source. The detailed table gives the raw multiple scatter corrupted moments and the f2, f3 correction factors along with the corrected moments.

We will now present the various comparisons with the spread sheet (Ref [13]):

Calibration curve: $D = a\, m/(1 + b\, m)$ where D is the Feynman Doubles and m is the ^{235}U linear density.

Mass defect for Unpoisoned Intact, Partial defect, Poisoned Intact Assemblies

Thermal Mode: Calibration

UNCL D = 10.53 m/(1 + .028 m)

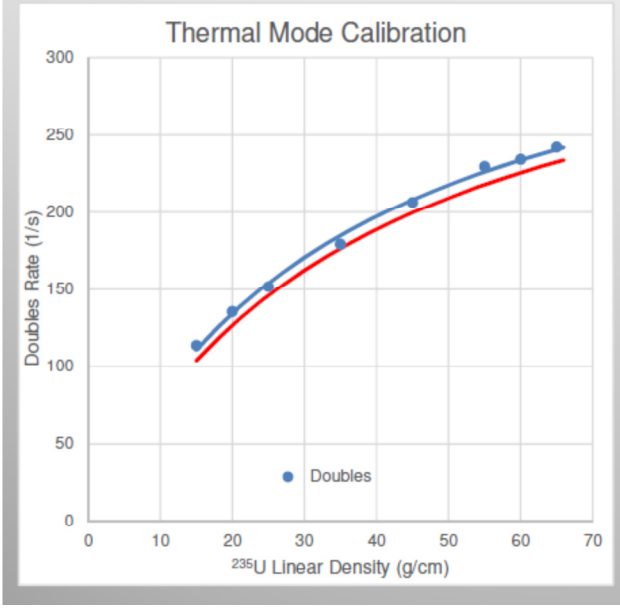

Stilbene D = 11.28 m/(1 + .057 m)

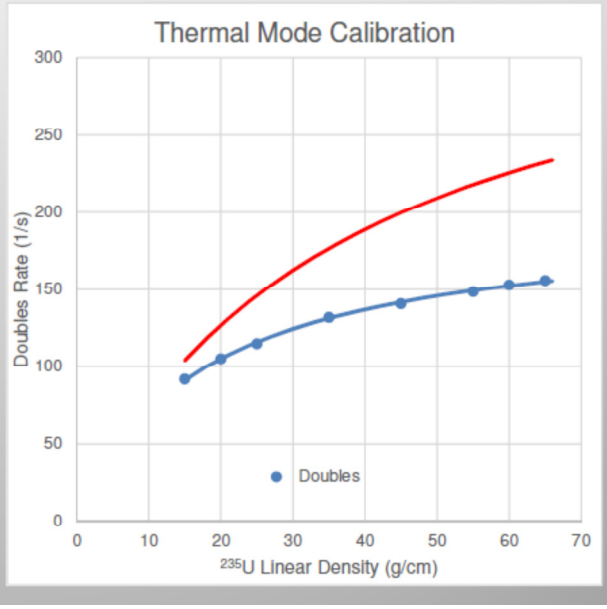

Thermal Mode: Unpoisoned Intact

UNCL(LD mass defect < 28.7%)

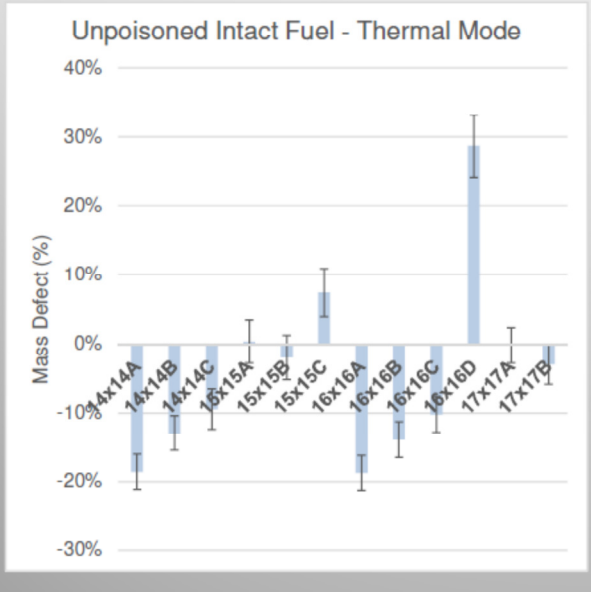

Stilbene (LD mass defect < 9.5%)

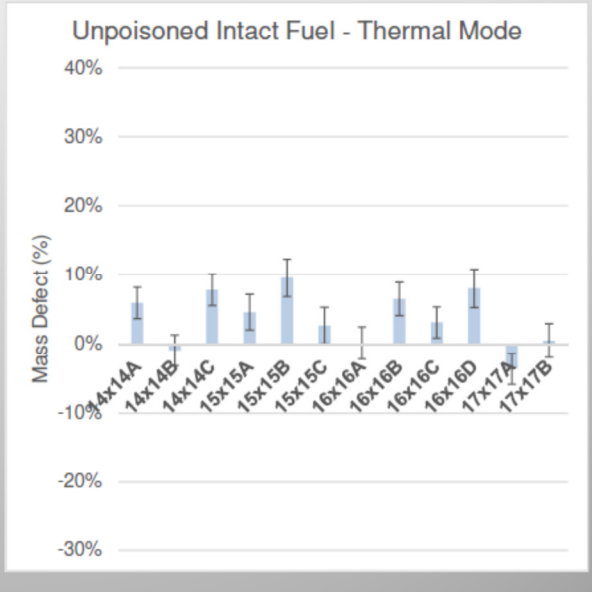

Thermal Mode: Partial Defect

UNCL (LD mass defect < 13.1%)

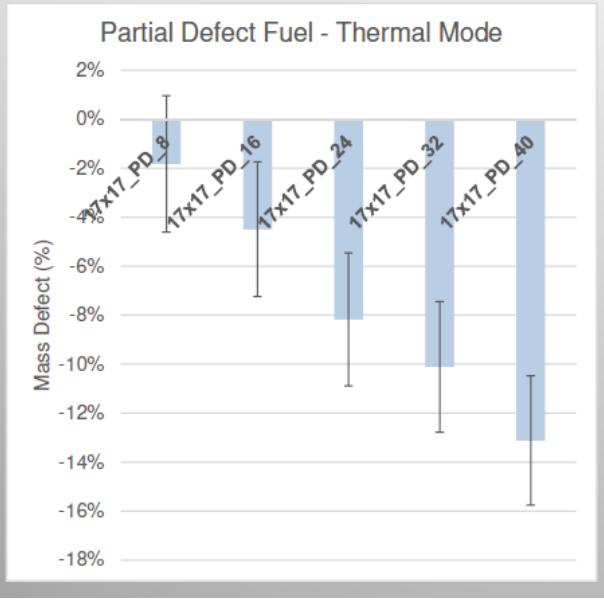

Stilbene (LD mass defect <13.7%)

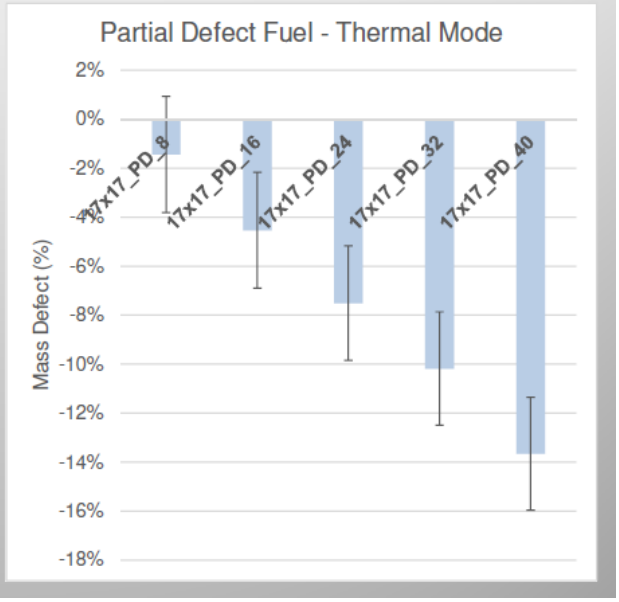

Thermal Mode: Poisoned Intact

UNCL (LD mass defect < 54%)

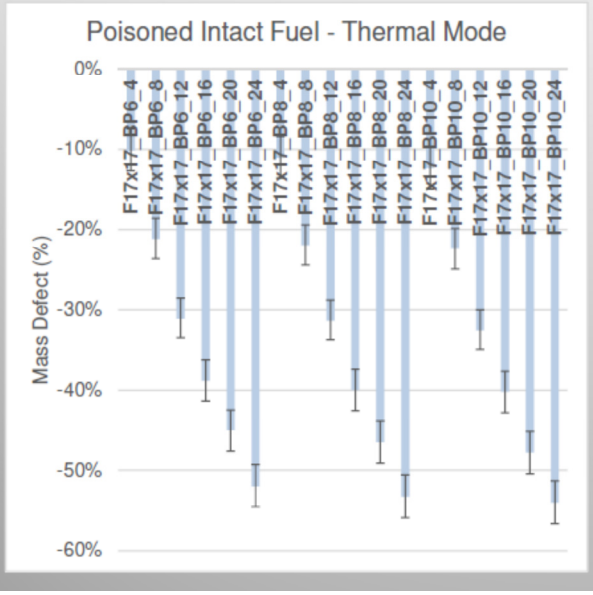

Stilbene (LD mass defect <56.7%)

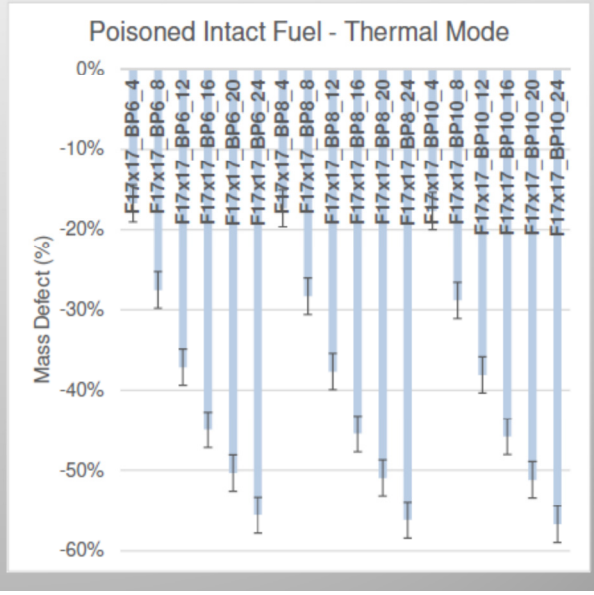

It is evident that in thermal mode the prototype stilbene collar performance is similar to that of the standard He-3 collar. Both collars perform poorly for the Gd poisoned assemblies because the Gd neutron absorption of thermal neutrons distorts the calibration curves which are based on calibration assemblies without any Gd poison. It is because of this that fast mode with Cd lining is necessary. The Cd lining filters out low energy neutrons below the Cd cutoff energy of 0.5 eV from entering the fuel assembly and therefore the Gd poison has a smaller effect on the corresponding calibration curves.

11. Fast Mode Simulation Results for Neutron Rodeo Project

We now show the corresponding simulation results in fast mode with a 0.5mm Cd cavity lining.

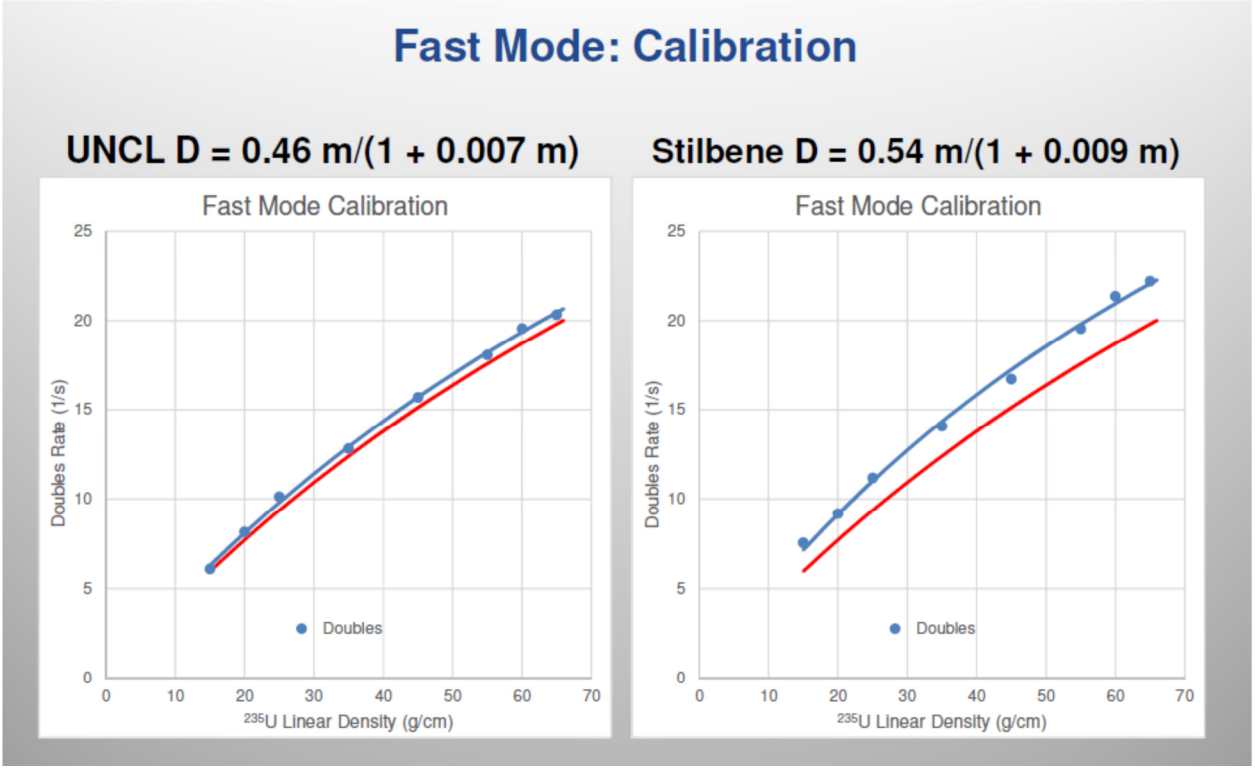

Fast Mode: Unpoisoned Intact

UNCL (LD mass defect < 9.1%)

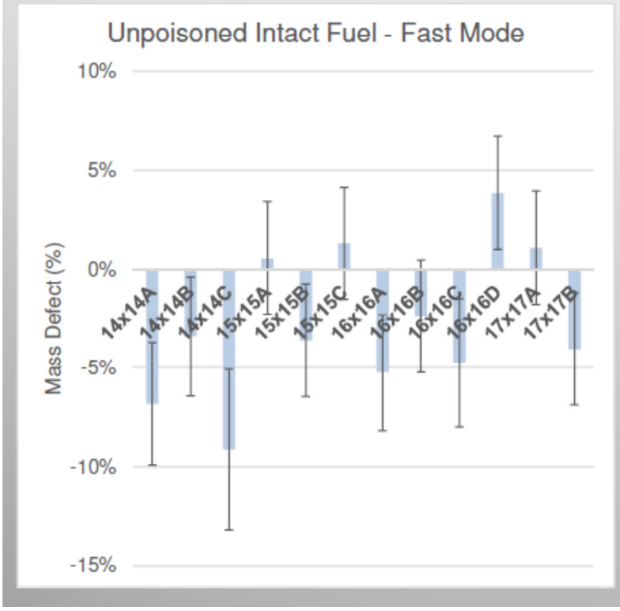

Stilbene (LD mass defect < 6.6%)

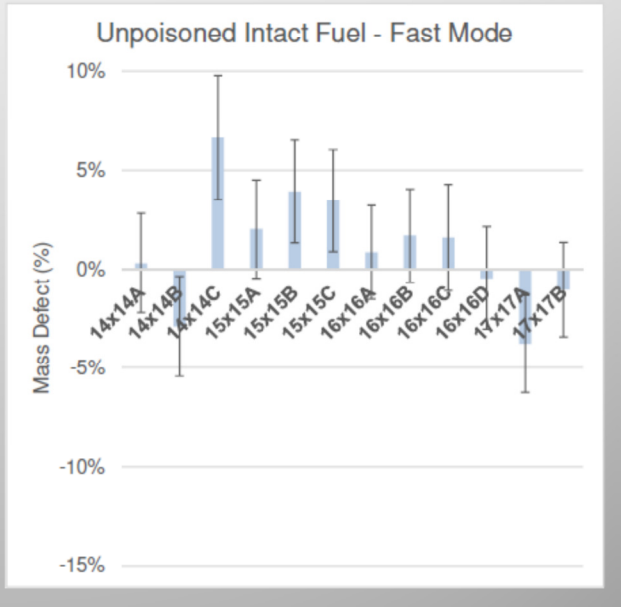

Fast Mode: Partial Defect

UNCL (LD mass defect < 13.5%)

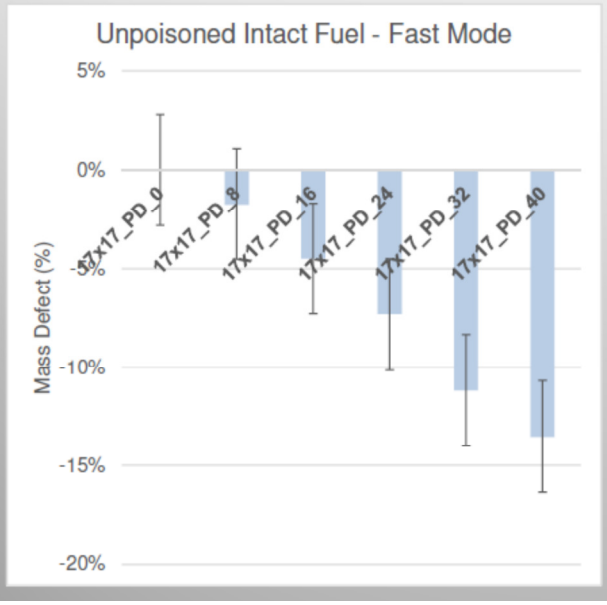

Stilbene (LD mass defect <15.9%)

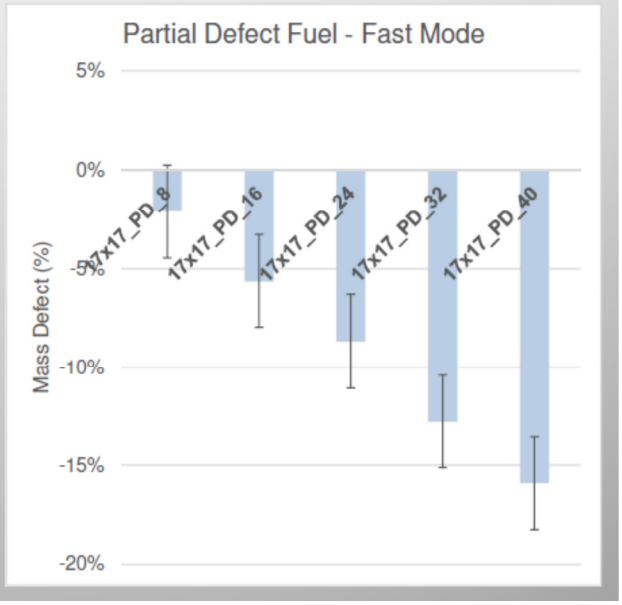

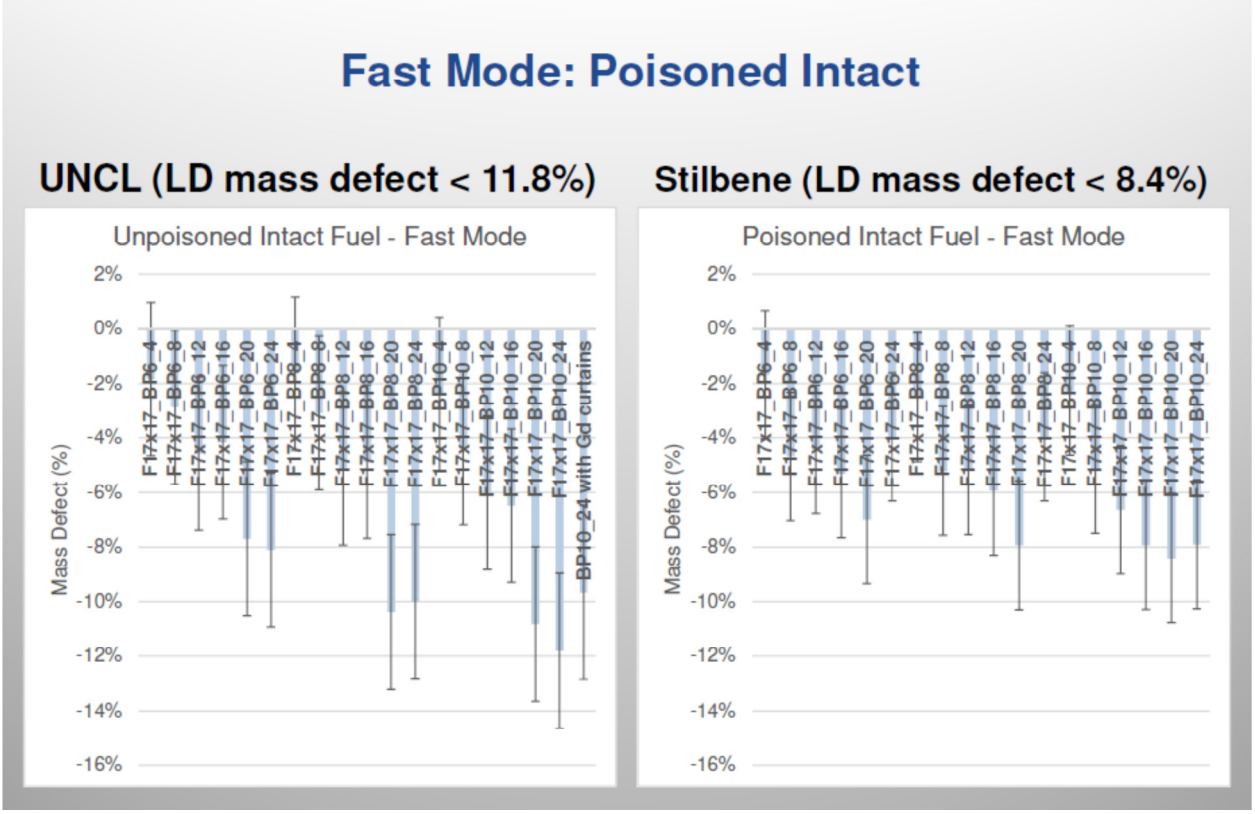

In fast mode it is evident that the prototype stilbene collar performance is significantly better that the standard He-3 collar. For the poisoned assemblies the reconstructed ^{235}U linear density is 30% better. The prototype stilbene neutron collar could be further optimized by tweaking the geometry and, in fast mode, making use of a bare AmLi interrogating source instead of a poly moderated AmLi source. While we have not done these optimization studies yet, we hope to look into this further at a later time.

12. Self-Consistent Assay

The traditional assay approach to neutron collar data, as described in Ref [1], is somewhat empirical through its use of calibration curves and several ad-hoc correction factors (k0,k1,…,k5). It would be desirable to have more fundamental assay methodology that would allow us to infer multiplication, efficiency and source (including alpha ratio) self-consistently.

Since the neutron collar has a nominal efficiency around 10% the count distributions from the list mode data will have significant triples with almost no

accidental triples in shift-register coincidence counting. This triples information contained in the data can be used for a self-consistent assay.

There are two methods to do a self-consistent assay. The first method is a general optimization code called Bigfit that was developed at LLNL to directly fit count distributions in order to determine SNM parameters that best fit the data. Bigfit is a robust optimization code but, as of yet, does not include the multiple scatter crosstalk correction factors f2 and f3. The second method, which is mathematically stable only for low multiplication M, is based on using the measured moments from the data to determine SNM parameters through the exact analytical 0-D point model formulas. This second method was first proposed by Hage and Cifarelli & Cifarelli and Hage in Ref [14, 15]. The first four Feynman moments in the 0-D point model are (Ref [10]):

$$R_1 = (\epsilon q M)\,(1 + A)\,S_f$$

$$R2F = (\epsilon q M)\left[\frac{D_{2\,s}}{(1 + A)} + (M - 1)\,D_2\right]$$

$$R3F = (\epsilon q M)^2\left[\frac{D_{3\,s}}{(1 + A)} + (M - 1)\left(\frac{2\,D_{2\,s}\,D_2}{(1 + A)} + D_3\right) + 2\,(M - 1)^2\,D_2^2\right]$$

$$R4F = (\epsilon q M)^3\left[\frac{D_{4\,s}}{(1 + A)} + (M - 1)\left(D_4 + 2\,\frac{D_3\,D_{2\,s}}{(1 + A)} + 3\,\frac{D_2\,D_{3\,s}}{(1 + A)}\right) + (M - 1)^2\left(5\,D_2\,D_3 + 5\,\frac{D_2^2\,D_{2\,s}}{(1 + A)}\right) + 5\,(M - 1)^3\,D_2^3\right]$$

where the various symbols have been defined in Section 6. The first three of these Feynman moments are related to singles, doubles, and triples though:

Singles = R1
Doubles = R1*R2F
Triples = R1*R3F

Fuel assemblies have low multiplication and therefore we can apply the Hage-Cifarelli (HC) algebra to infer multiplication M, efficiency ε, and source S_f along

with alpha ratio A. The prototype stilbene neutron collar is especially suited for a HC assay in thermal mode. This is because stilbene is (almost) blind to the low energy moderated AmLi interrogating source neutrons. For the Obninsk AmLi source there may be a few neutrons that can directly shine on and be detected by the stilbene cells because of the bump at 2 MeV in its neutron energy spectrum as discussed in Section 3. The LLNL code Bigfit takes into account any direct shine but for the HC algebra we can ignore it to a good approximation.

In thermal mode, from the point of view of the stilbene cells, the source of neutrons is the 1st generation of fission neutrons created from the induced fission of ^{235}U by the thermalized (moderated by poly bank) AmLi interrogating neutrons. The cross section for thermal neutrons inducing fission on ^{235}U is very large at 580 b. Furthermore, from the perspective of the stilbene cells, the alpha ratio A is effectively 0 as there are no random source of neutrons that it can see. This is a dramatic simplification from using stilbene. By contrast, a He-3 based neutron collar will have a significant alpha ratio A > 0 since the He-3 detector will clearly see the random thermalized AmLi interrogating neutron source.

The use of stilbene neutron collar therefore greatly simplifies the HC algebra to a system of 3 equations for singles, doubles and triples that can be solved for multiplication M, efficiency ε and source S_f. By contrast, a He-3 based neutron collar with its significant alpha ratio A > 0 would require using Quads (R1*R4F) to determine A but even at 10% efficiency the quads will most probably be very small in magnitude and unreliable because of low multiplication. Ref [16] discusses the active multiplicity equations based on the HC method in the context of He-3 neutron detectors.

The fast 1st generation fission neutrons multiply by subsequently inducing fission on both ^{235}U and ^{238}U. In the HC algebra above, D_{2S},D_{3S} will be Diven's constants for thermal neutron induced fission of ^{235}U while D_2 and D_3 will be Diven's constants for fast neutron induced fission of ^{235}U and ^{238}U.

The HC algebra will produce a total multiplication M from which the net multiplication (qM) can be computed. This HC net multiplication qM can then be compared directly to the MCNPX simulation value for the net multiplication. Table

3 in the Appendix shows the HC net M is within 1%-7% of MCNPX value of net M for the set of fuel assemblies modeled in the neutron rodeo project. The table shows the HC effective point model efficiency for the prototype stilbene neutron collar with the fuel assemblies is around 9%. The HC source, in units of neutrons/s, scales with the linear ^{235}U mass density and decreases according to the Gd poison content. What is needed is a conversion/coupling factor to convert the HC source to ^{235}U linear mass density. This will require a detailed MCNP study of how the AmLi neutrons couple to the ^{235}U fuel component, which we hope to do in the near future.

In thermal mode the main challenge is to assay fuel assemblies with Gd poison that absorb thermal neutrons resulting in a loss of correlation contained in those neutrons. However, one can can detect the Gd(n,gamma) capture lines whereby the lost correlation information in captured neutrons can be recovered through the capture gamma lines. In principle, with list mode data for both neutrons and gammas the capture gamma lines can be used effectively in the assay process. In practice, this would require detectors that can efficiently detect capture gamma lines.

A self-consistent assay methodology that complements the current traditional methodology would be both useful and desirable. At a nominal efficiency of 10% there is considerable information in the neutron data (e.g., triples) that can be used towards a self-consistent assay.

Summary

A neutron collar using stilbene organic scintillator cells for fast neutron counting was described for the assay of fresh low enriched uranium (LEU) fuel assemblies.

The prototype stilbene collar has several benefits compared to He-3 based collars. First, because it is a threshold detector, it is not blinded by the thermalized AmLi interrogating neutron source and is able to clearly see the fission signal from the fuel assembly. Second, its fast response times (nanoseconds vs microseconds) allows fission chains to be resolved with much shorter measurement timegates and therefore much fewer 'accidentals' in those shorter timegates. Third, it permits an unfolding of the neutron energy spectrum of the fuel assembly from the measured scintillator light output spectrum.

Stilbene has the highest organic scintillation efficiency with much higher light yield than plastics or liquids. Stilbene's excellent PSD implies excellent gamma rejection which in turn implies high neutron efficiency. The prototype stilbene collar can operate at a PSD threshold of 60 keVee which we have shown makes it competitive with He-3 collars in efficiency, particularly in fast mode with a Cd lining. Indeed in fast mode the prototype stilbene collar performed 30% better in predicting ^{235}U linear mass density compared to standard He-3 UNCL collar for fuel assemblies with Gd burnable poison.

A self-consistent assay methodology, uniquely suited to the stilbene collar, using triples was described which complements traditional assay based on doubles calibration curves. In particular, we showed that we could correctly assay the net multiplication of the fuel assemblies when compared to the calculated MCNP net multiplication. This self-consistent assay, feasible in both passive and active modes, can potentially provide key insights towards a more robust assay.

Stilbene, like all scintillator detectors, is vulnerable to neutron multiple scatter crosstalk and also pulse pileup from high gamma background. With respect to neutron crosstalk, we have developed a physics model driven optimization algorithm to infer both the neutron energy spectrum and the crosstalk correction factors simultaneously from the measured scintillation light output spectrum.

With respect to high gamma background from SNM alpha decay, we expect to filter out these gammas with lead/bismuth shielding in hardware, low energy cuts in our modeling, along with pileup rejection algorithms in the data acquisition pipeline. Any remaining gammas that get misidentified as neutrons can be modeled as an effective alpha ratio A.

Acknowledgements

We would like to thank Arden Dougan and Anthony Belian from the NA-241 program office of Safeguards Technology for letting us participate in the FY16 Advanced Neutron Detector Rodeo Project.

This work was performed under the auspices of the U.S. Department of Energy by Lawrence Livermore National Laboratory under Contract DE-AC52-07NA27344.

References

1. "Neutron Collar Calibration and Evaluation for Assay of LWR Fuel Assemblies Containing Burnable Neutron Absorbers," H.O. Menlove, J. E. Stewart, S. Z. Qiao, T. R. Wenz and G.P.D. Verrecchia, Los Alamos National Laboratory Report LA-11965-MS November 1990.
2. Canberra. 2011. Model JCC-71, 72 and 73 Neutron Coincidence Collars, http://www.canberra.com/products/waste_safeguard_systems/pdf/JCC-71-72-73-SS-C38898.pdf
3. "Scintillation properties of solution-grown trans-stilbene single crystals," Natalia Zaitseva, Andrew Glenn, Leslie Carman, H. Paul Martinez, Robert Hatarik, Helmut Klapper, and Stephen Payne, Nuclear Instruments and Methods in Physics Research A, 789, 8-15 (2015).
4. "Application of solution techniques for rapid growth of organic crystals," N. Zaitseva, L. Carman, A. Glenn, J. Newby, M. Faust, S. Hamel, N. Cherepy, S. Payne, J. Crystal Growth, 314(2011) 163, US Patent Pub. No. US 2010/0252741 held by Zaitseva et al.
5. http://www.inradoptics.com/products/scintillation-crystals/stilbene-single-crystals
6. "State of the Art Monte Carlo Modeling of Active Collar Measurements and Comparison with Experiment," S. Croft, A. Favalli, M. T. Swinhoe, and Carlos D. Rael, Los Alamos National Laboratory Report LA-UR-11-03760, July 2011.
7. "Determination of light output function and angle dependent correction for a stilbene crystal scintillation neutron spectrometer," W. Hansen and D. Richter, Nuclear Instruments and Methods in Physics Research A, 476, 195-199 (2002).
8. "Time Interval Distributions and the Rossi Correlation Function," M. Prasad, N. Snyderman, J. Verbeke, and R. Wurtz, Nuclear Science and Engineering, 174, 1-29 (2013).
9. "Customized MCNPX to Generate "List-Mode" ^{3}He Neutron Captures and Scintillator Counts," J. M. Verbeke, LLNL-TM-671194, Lawrence Livermore National Laboratory (2015).
10. "Notes on Fission Chain Theory and its Implementation in Bigfit & NMAC," Manoj K. Prasad, LLNL-PRES-483092 Lawrence Livermore National

Laboratory (2011) & LLNL-PRES-691259 Lawrence Livermore National Laboratory (2016).
11. “Neutron crosstalk between liquid scintillators,” J. M. Verbeke, M. K. Prasad, and N. J. Snyderman, Nuclear Instruments and Methods in Physics Research A, 794, 127-140 (2015).
12. “Method for measuring multiple scattering corrections between liquid scintillators,” J. M. Verbeke, A. M. Glenn, G. J. Keefer, R. E. Wurtz, Nuclear Instruments and Methods in Physics Research A, 825, 69-77 (2016).
13. Anthony Belian, private communication.
14. “Correlation Analysis with Neutron Count Distributions in Randomly or Signal Triggered Intervals for Assay of Special Fissile Materials,” W. Hage and D. M. Cifarelli, Nuclear Science and Engineering, 89, 159-176 (1985).
15. “Models for a Three-Parameter Analysis of Neutron Signal Correlation Measurements for Fissile Material,” D. M. Cifarelli and W. Hage, Nuclear Instruments and Methods in Physics Research A, 251, 550-563 (1986).
16. “Active Neutron Multiplicity Counting,” N. Ensslin, W. H. Geist, M. S. Krick, and M. M. Pickrell, Passive Nondestructive Assay of Nuclear Materials, 2007 Addendum, Los Alamos National Laboratory 2007.

Appendix

Simulation Results for Die-Away Time, f2/f3, Raw & Corrected (R1,R2F,R3F), and Doubles Stilbene Neutron Collar @ 60 keVee Threshold in Thermal Mode

Fuel Assembly	U5LD(g/cm)	LTime(ns)	Raw R1	Raw R2F	Raw R3F	f2	f3	Corr R1	Corr R2F	Corr R3F	Doubles
17x17_BP6_4	51.500000	8.582607	1214.699058	0.141110	0.016578	0.020974	0.000193	1189.295702	0.117408	0.010855	139.739358
17x17_BP6_8	51.200000	8.499407	1169.575283	0.140295	0.016408	0.020912	0.000192	1145.187372	0.116769	0.010739	138.722065
17x17_BP6_12	50.900000	8.332912	1122.986755	0.139182	0.016267	0.020902	0.000192	1099.581072	0.115689	0.010651	127.209619
17x17_BP6_16	50.600000	8.439040	1079.692922	0.137789	0.015981	0.020874	0.000189	1057.224781	0.114364	0.010443	120.908225
17x17_BP6_20	50.300000	8.464556	1042.786372	0.136746	0.015973	0.020810	0.000189	1021.150240	0.113410	0.010490	115.808368
17x17_BP6_24	49.900000	8.170743	996.736476	0.136027	0.015540	0.020788	0.000178	976.097863	0.112762	0.010125	110.067306
17x17_BP8_4	51.500000	8.545419	1213.079966	0.141008	0.016559	0.020971	0.000193	1187.713959	0.117401	0.010842	139.439288
17x17_BP8_8	51.200000	8.676702	1166.652817	0.140189	0.016374	0.020908	0.000193	1142.328083	0.116666	0.010711	133.270482
17x17_BP8_12	50.900000	8.552871	1120.168174	0.139130	0.016265	0.020899	0.000192	1096.824459	0.115641	0.010652	126.838072
17x17_BP8_16	50.500000	8.512278	1076.248467	0.137633	0.015862	0.020846	0.000191	1053.876771	0.114234	0.010338	120.388813
17x17_BP8_20	50.200000	8.685660	1038.414352	0.136556	0.015929	0.020813	0.000187	1016.869929	0.113227	0.010457	115.136732
17x17_BP8_24	49.900000	8.195120	990.624261	0.135991	0.015635	0.020765	0.000177	970.135960	0.112755	0.010223	109.387301
17x17_BP10_4	51.500000	8.539182	1212.035926	0.140971	0.016605	0.020972	0.000193	1186.690588	0.117364	0.010888	139.275310
17x17_BP10_8	51.200000	8.628665	1164.980089	0.140092	0.016376	0.020912	0.000192	1140.687997	0.116570	0.010717	132.969925
17x17_BP10_12	50.800000	8.332322	1117.219832	0.139055	0.016105	0.020887	0.000193	1093.948271	0.115578	0.010503	126.436117
17x17_BP10_16	50.500000	8.444156	1073.206966	0.137670	0.015873	0.020846	0.000192	1050.896434	0.114268	0.010345	120.083479
17x17_BP10_20	50.200000	8.624934	1035.071398	0.136694	0.015977	0.020808	0.000187	1013.601295	0.113366	0.010500	114.908404
17x17_BP10_24	49.800000	8.043276	986.839594	0.135729	0.015511	0.020773	0.000178	966.420104	0.112486	0.010112	108.708678
17x17_cal_15	15.000000	8.774393	813.057661	0.138091	0.015936	0.020439	0.000167	796.511723	0.115184	0.010508	91.745446
17x17_cal_20	20.000000	6.928892	919.885865	0.139755	0.016053	0.020610	0.000175	901.000887	0.116610	0.010507	105.065755
17x17_cal_25	25.000000	8.557711	1003.118371	0.140230	0.016154	0.020771	0.000167	982.385133	0.116930	0.010565	114.870549
17x17_cal_35	35.000000	8.014982	1131.792500	0.142477	0.016635	0.020881	0.000180	1108.252117	0.118974	0.010894	131.853310
17x17_cal_45	45.000000	7.903355	1216.042426	0.141659	0.016526	0.020925	0.000195	1190.663435	0.118081	0.010790	140.594654
17x17_cal_55	55.000000	8.354922	1281.091272	0.142164	0.016716	0.021051	0.000191	1254.209798	0.118455	0.010933	148.567809
17x17_cal_60	60.000000	9.059790	1311.662189	0.142799	0.016958	0.021122	0.000199	1284.038592	0.118984	0.011122	152.791152
17x17_cal_65	65.000000	8.017045	1336.333085	0.142907	0.016966	0.021117	0.000193	1308.202800	0.119106	0.011125	155.815296
14x14C	19.780000	7.418816	947.527795	0.139970	0.015541	0.020855	0.000172	927.858131	0.116572	0.009964	108.161972
16x16C	30.950000	8.167928	1099.001095	0.141590	0.016230	0.020888	0.000172	1076.152231	0.118123	0.010552	127.117822
14x14B	37.310000	8.233058	1153.870916	0.141847	0.016473	0.021007	0.000180	1129.731934	0.118224	0.010738	133.561785
14x14A	37.570000	8.049189	1177.092449	0.142458	0.016405	0.021193	0.000185	1152.246556	0.118611	0.010603	136.669113
17x17A	41.290000	7.228803	1188.608150	0.141049	0.016609	0.020956	0.000196	1163.764114	0.117448	0.010886	136.681800
16x16A	46.900000	8.258745	1235.840092	0.142265	0.016397	0.021113	0.000197	1209.820483	0.118470	0.010601	143.327767
16x16B	50.160000	8.436733	1271.064889	0.142992	0.016627	0.021208	0.000192	1244.200120	0.119097	0.010780	148.180832
17x17B	54.820000	8.645423	1281.302850	0.142669	0.017059	0.020997	0.000192	1254.480797	0.119003	0.011250	149.287366
15x15A	58.370000	8.171724	1305.518620	0.143489	0.017333	0.021169	0.000192	1277.974437	0.119624	0.011444	152.876574
15x15C	60.910000	8.219482	1313.944237	0.143248	0.017203	0.021081	0.000193	1286.330579	0.119478	0.011346	153.688042
15x15B	61.540000	7.972909	1334.099371	0.143366	0.017012	0.021100	0.000196	1306.030170	0.119565	0.011149	156.155541
16x16D	64.070000	9.155723	1340.925221	0.143107	0.017169	0.020900	0.000183	1313.002901	0.119562	0.011372	156.984762
17x17_PD_40	44.400000	8.920146	1211.463250	0.141895	0.016465	0.020954	0.000193	1186.150792	0.118288	0.010720	140.307468
17x17_PD_32	45.900000	8.588575	1224.513584	0.142017	0.016475	0.021003	0.000195	1198.866238	0.118349	0.010711	141.884665
17x17_PD_24	47.400000	8.419027	1234.525191	0.141972	0.016701	0.020979	0.000195	1208.696554	0.118331	0.010935	143.025998
17x17_PD_16	48.900000	8.509210	1245.069808	0.141986	0.016779	0.021002	0.000189	1219.007518	0.118338	0.011013	144.255184
17x17_PD_8	50.400000	8.930731	1252.669034	0.142258	0.016863	0.021005	0.000188	1226.446384	0.118605	0.011083	145.462589
17x17_PD_0	51.900000	8.789622	1259.053654	0.142085	0.016702	0.020997	0.000188	1232.707007	0.118443	0.010938	146.006086
UNCL_15x15	23.800000	7.992563	962.988260	0.139543	0.015767	0.020646	0.000175	943.185145	0.116364	0.010234	109.753045
pass_17x17_cal_55	55.000000	11.881633	130.667456	0.129633	0.013098	0.020255	0.000154	128.034678	0.107131	0.008169	13.716460
EMPTY_CAVITY	0.000000	10.994696	169.630229	0.014846	0.000117	0.010860	0.000018	167.801860	0.004006	0.000011	0.672290
Cf34000	0.000000	4.492839	5399.571814	0.270620	0.045100	0.027968	0.000311	5249.488925	0.235781	0.029460	1237.731469

Table 1: Simulation results for thermal mode

Simulation Results for Die-Away Time, f2/f3, Raw & Corrected (R1,R2F,R3F), and Doubles Stilbene Neutron Collar @ 60 keVee Threshold in Fast Mode

Fuel Assembly	USLD(g/cm)	LTime(ns)	Raw R1	Raw R2F	Raw R3F	f2	f3	Corr R1	Corr R2F	Corr R3F	Doubles
17x17_BP6_4	51.500000	7.792289	234.809704	0.099534	0.011718	0.016970	0.000125	230.834730	0.081086	0.008487	18.717533
17x17_BP6_8	51.200000	7.477035	232.699060	0.098139	0.011482	0.016927	0.000116	228.773535	0.079787	0.008323	18.253104
17x17_BP6_12	50.900000	6.989507	231.309070	0.098395	0.010945	0.016912	0.000109	227.413477	0.080074	0.007808	18.269962
17x17_BP6_16	50.600000	7.091264	229.978399	0.097984	0.011304	0.016874	0.000112	226.112330	0.079701	0.008169	18.021266
17x17_BP6_20	50.300000	7.783599	228.517620	0.097113	0.010559	0.016853	0.000111	224.681188	0.078869	0.007482	17.720383
17x17_BP6_24	49.900000	8.201844	227.419672	0.098811	0.011858	0.016800	0.000114	223.612007	0.080584	0.008685	18.019585
17x17_BP8_4	51.500000	7.597276	234.229561	0.099243	0.011629	0.016964	0.000121	230.267577	0.080819	0.008417	18.609915
17x17_BP8_8	51.200000	7.511638	231.790326	0.098116	0.011598	0.016918	0.000113	227.883491	0.079783	0.008442	18.181126
17x17_BP8_12	50.900000	6.579629	230.301638	0.098326	0.010971	0.016919	0.000111	226.420563	0.079993	0.007831	18.112172
17x17_BP8_16	50.500000	6.545198	228.718328	0.097921	0.011599	0.016846	0.000112	224.879633	0.079668	0.008460	17.915605
17x17_BP8_20	50.200000	8.009753	227.238876	0.096836	0.010411	0.016785	0.000115	223.487094	0.078655	0.007351	17.574383
17x17_BP8_24	49.900000	8.164578	225.297915	0.097824	0.011509	0.016737	0.000117	221.538190	0.079669	0.008384	17.649730
17x17_BP10_4	51.500000	7.648882	233.992524	0.099454	0.011938	0.016957	0.000121	230.036133	0.081033	0.008710	18.640542
17x17_BP10_8	51.200000	7.113552	231.248273	0.098339	0.011894	0.016911	0.000113	227.352139	0.080008	0.008721	18.190101
17x17_BP10_12	50.800000	6.787654	229.424080	0.097602	0.010831	0.016885	0.000112	225.564890	0.079314	0.007722	17.890381
17x17_BP10_16	50.500000	7.138559	227.614185	0.097073	0.011290	0.016841	0.000111	223.795562	0.078842	0.008191	17.644393
17x17_BP10_20	50.200000	7.264429	226.139856	0.096907	0.010631	0.016772	0.000116	222.358866	0.078735	0.007562	17.507345
17x17_BP10_24	49.800000	7.619621	223.872742	0.097528	0.011768	0.016734	0.000115	220.158815	0.079387	0.008647	17.476160
17x17_cal_15	15.000000	7.921032	152.159277	0.065398	0.006817	0.014226	0.000078	150.001949	0.050418	0.005133	7.562734
17x17_cal_20	20.000000	9.835197	165.377399	0.072124	0.008012	0.014870	0.000084	162.927298	0.056379	0.006041	9.183625
17x17_cal_25	25.000000	8.024114	178.498443	0.079977	0.008937	0.015276	0.000103	175.777063	0.063645	0.006644	11.187269
17x17_cal_35	35.000000	9.407586	201.405413	0.088526	0.009592	0.016224	0.000106	198.148642	0.071083	0.006908	14.085078
17x17_cal_45	45.000000	8.825831	223.302403	0.094244	0.010312	0.016726	0.000112	219.580514	0.076175	0.007351	16.726595
17x17_cal_55	55.000000	9.195170	242.600436	0.100601	0.011867	0.017107	0.000133	238.457710	0.081070	0.008567	19.546274
17x17_cal_60	60.000000	7.607015	251.060143	0.105136	0.012544	0.017331	0.000123	247.607939	0.086226	0.009050	21.350359
17x17_cal_65	65.000000	8.340990	260.823358	0.105635	0.012141	0.017372	0.000131	256.303698	0.086650	0.008627	22.208616
14x14C	19.780000	6.114594	182.363882	0.068731	0.006806	0.014697	0.000080	179.696137	0.053222	0.004988	9.563821
16x16C	30.950000	6.360998	201.958442	0.083326	0.009035	0.015770	0.000101	198.783473	0.066444	0.006588	13.208017
14x14B	37.310000	8.325737	212.619479	0.087720	0.009723	0.016154	0.000108	209.194958	0.070355	0.007065	14.717994
14x14A	37.370000	7.985340	225.649692	0.085615	0.009095	0.016160	0.000111	222.012681	0.068270	0.006519	15.156715
17x17A	41.290000	9.233116	216.388006	0.091882	0.010119	0.016528	0.000113	212.822380	0.074052	0.007264	15.759877
16x16A	46.900000	10.153008	242.004949	0.093023	0.010393	0.016661	0.000115	237.985142	0.075032	0.007474	17.856516
16x16B	50.160000	7.045244	243.125005	0.097123	0.010468	0.017012	0.000113	239.005036	0.078709	0.007369	18.811931
17x17B	54.820000	8.139007	241.967124	0.101107	0.012183	0.017117	0.000131	237.833810	0.082463	0.008856	19.612563
15x15A	58.370000	10.262897	249.435890	0.103956	0.012231	0.017327	0.000126	245.126806	0.085062	0.008783	20.850920
15x15C	60.910000	9.490440	253.219336	0.105798	0.012123	0.017299	0.000132	248.848805	0.086883	0.008613	21.620608
15x15B	61.540000	9.241350	258.096788	0.105001	0.012134	0.017351	0.000133	253.628612	0.086042	0.008642	21.822774
16x16D	64.070000	8.387092	250.010721	0.107707	0.012987	0.017384	0.000131	245.675531	0.088674	0.009372	21.785007
17x17_PD_40	44.400000	8.061816	222.152821	0.094533	0.010264	0.016672	0.000114	218.460833	0.076509	0.007300	16.714228
17x17_PD_32	45.900000	7.856247	225.096711	0.095587	0.010378	0.016744	0.000111	221.341433	0.077481	0.007371	17.149697
17x17_PD_24	47.400000	7.630958	228.137975	0.097196	0.010887	0.016817	0.000119	224.312328	0.078964	0.007790	17.712541
17x17_PD_16	48.900000	7.704194	231.095604	0.098077	0.011016	0.016801	0.000113	227.204277	0.079761	0.007882	18.121980
17x17_PD_8	50.400000	7.675058	233.778811	0.099235	0.011337	0.016926	0.000113	229.836653	0.080874	0.008151	18.587768
17x17_PD_0	51.900000	8.349455	236.374427	0.099695	0.011607	0.017037	0.000128	232.356290	0.081166	0.008361	18.859542
UNCL_15x15	23.800000	9.403424	176.476836	0.075731	0.008346	0.015053	0.000100	173.825476	0.059698	0.006223	10.377029
pass_17x17_cal_55	55.000000	8.894402	120.029760	0.127018	0.013161	0.020058	0.000147	117.635639	0.104795	0.008376	12.327864
EMPTY_CAVITY	0.000000	8.676371	166.063043	0.015097	0.000049	0.011020	0.000030	164.243228	0.004064	-0.000070	0.667464
Cf34000	0.000000	4.400001	5383.180429	0.270046	0.044869	0.027933	0.000305	5233.792296	0.235283	0.029301	1231.420051

Table 2: Simulation results for fast mode

HC Algebra Results for Net Multiplication, Efficiency, and Source
Stilbene Neutron Collar with 45 Fuel Assemblies @ 60 keVee in Thermal Mode

Fuel Assembly	U5LD(g/cm)	MCNP Net M	HC Net M (Error)	HC Eff	HC Source (n/s)
17x17_BP6_4	51.500000	1.194200	1.127683(5.570010%)	8.871805%	11887.509401
17x17_BP6_8	51.200000	1.186900	1.128457(4.924020%)	8.801019%	11530.779644
17x17_BP6_12	50.900000	1.179300	1.133120(3.915864%)	8.626484%	11249.090841
17x17_BP6_16	50.600000	1.173000	1.134655(3.268999%)	8.497681%	10964.863610
17x17_BP6_20	50.300000	1.166500	1.144745(1.865001%)	8.235236%	10831.906993
17x17_BP6_24	49.900000	1.158900	1.133386(2.201564%)	8.403128%	10248.835712
17x17_BP8_4	51.500000	1.194000	1.127882(5.537494%)	8.860458%	11884.800353
17x17_BP8_8	51.200000	1.186500	1.128056(4.925771%)	8.801404%	11505.575979
17x17_BP8_12	50.900000	1.178800	1.133573(3.836729%)	8.613952%	11232.729760
17x17_BP8_16	50.500000	1.172300	1.131071(3.516970%)	8.558244%	10887.182228
17x17_BP8_20	50.200000	1.165800	1.144788(1.802400%)	8.221141%	10804.592236
17x17_BP8_24	49.900000	1.158000	1.137950(1.731408%)	8.315171%	10252.696856
17x17_BP10_4	51.500000	1.193900	1.130040(5.348835%)	8.813653%	11914.823654
17x17_BP10_8	51.200000	1.186300	1.129045(4.826341%)	8.774107%	11514.701051
17x17_BP10_12	50.800000	1.178400	1.127654(4.306309%)	8.727423%	11115.646041
17x17_BP10_16	50.500000	1.171800	1.131110(3.472429%)	8.559969%	10853.826648
17x17_BP10_20	50.200000	1.165200	1.145542(1.687115%)	8.217255%	10767.861853
17x17_BP10_24	49.800000	1.157400	1.135058(1.930321%)	8.350417%	10196.228669
17x17_cal_15	15.000000	1.117000	1.130941(-1.248107%)	8.631970%	8159.098603
17x17_cal_20	20.000000	1.135800	1.120074(1.384553%)	8.961797%	8976.009701
17x17_cal_25	25.000000	1.151000	1.120063(2.687800%)	8.986633%	9759.827789
17x17_cal_35	35.000000	1.174200	1.118347(4.756660%)	9.180447%	10794.388249
17x17_cal_45	45.000000	1.191400	1.120728(5.931828%)	9.061005%	11724.986779
17x17_cal_55	55.000000	1.204700	1.123659(6.727033%)	9.027022%	12363.677588
17x17_cal_60	60.000000	1.210500	1.127282(6.874709%)	8.993124%	12666.077803
17x17_cal_65	65.000000	1.215900	1.126506(7.352079%)	9.017802%	12877.775034
14x14C	19.780000	1.130200	1.098836(2.775048%)	9.420303%	8963.624304
16x16C	30.950000	1.161700	1.111058(4.359289%)	9.272171%	10446.131374
14x14B	37.310000	1.174500	1.117626(4.842437%)	9.138009%	11061.843043
14x14A	37.570000	1.169900	1.109663(5.148864%)	9.341237%	11116.030589
17x17A	41.290000	1.186000	1.129351(4.776481%)	8.833963%	11664.885714
16x16A	46.900000	1.184600	1.110552(6.250888%)	9.310587%	11700.514981
16x16B	50.160000	1.194200	1.113081(6.792733%)	9.304211%	12013.894749
17x17B	54.820000	1.203700	1.132330(5.929195%)	8.889730%	12462.418317
15x15A	58.370000	1.208300	1.135393(6.033826%)	8.873512%	12684.703609
15x15C	60.910000	1.212800	1.132553(6.616674%)	8.920613%	12732.080818
15x15B	61.540000	1.212000	1.124077(7.254338%)	9.103655%	12762.660086
16x16D	64.070000	1.222800	1.132981(7.345346%)	8.918088%	12994.850070
17x17_PD_40	44.400000	1.191300	1.116431(6.284607%)	9.168547%	11587.968503
17x17_PD_32	45.900000	1.193700	1.115648(6.538648%)	9.190143%	11692.872158
17x17_PD_24	47.400000	1.195800	1.124666(5.948652%)	8.997375%	11944.771979
17x17_PD_16	48.900000	1.197800	1.127769(5.846626%)	8.933499%	12099.421290
17x17_PD_8	50.400000	1.199200	1.128594(5.887765%)	8.936584%	12160.160616
17x17_PD_0	51.900000	1.200600	1.123965(6.383031%)	9.020607%	12158.253551
UNCL_15x15	23.800000	1.142000	1.110818(2.730456%)	9.139329%	9290.512219

Table 3. HC algebra results for net multiplication qM, efficiency ε and source Sf for the set of fuel assemblies modeled in the neutron rodeo project. In particular the net M is compared to MCNP value for net M.